JOURNAL OF INFORMATION SCIENCE AND ENGINEERING 25, 793-805 (2009)

Simulated Annealing for Pattern Detection and Seismic Applications*

KOU-YUAN HUANG AND KAI-JU CHEN
Department of Computer Science
Chiao Tung University
Hsinchu, 300 Taiwan

Simulated annealing (SA) is adopted to detect the parameters of circles, ellipses, hyperbolas, and to treat lines as asymptotes of hyperbola in image. Also, the algorithm is applied to seismic pattern detection. We use the general equation for ellipses and hyperbolas in detection and define the distance from a point to a pattern such that the detection becomes feasible. The system error between N points and K patterns is defined. The proposed simulated annealing parameter detection system has the capability of searching a set of parameter vectors with global minimal error with respect to the input data. Experiments on the detection of circles, ellipses, hyperbolas, and lines in images are quite successful. The detection system is also applied to detect the line pattern of direct wave and the hyperbolic pattern of reflection wave in the simulated and real one-shot seismogram. The results can improve seismic interpretations and further seismic data processing.

Keywords: simulated annealing, global optimization, seismic pattern recognition, reflection wave, Hough transform, hyperbolic pattern detection

1. INTRODUCTION

Traditionally, parametric pattern detection was accomplished by Hough transform (HT), which mapped the points in image space to the parameter space and found the peaks in parameter space [1]. The coordinates of a peak in parameter space represented a pattern in image space.

Seismic pattern detection plays an important role in oil exploration. In one-shot seismic data, a line in the travel-time figure represents a direct wave and a hyperbola in the travel-time figure represents a reflection wave [2-4]. In 1985, Huang *et al.* had applied HT to detect line pattern of direct wave and hyperbolic pattern of reflection wave [5]. However, peak determination was not easy and memory requirement was also a problem.

In 2002, Hough transform neural network (HTNN) was proposed to the parameter detection by neural network method [6]. The competitive network minimized the distance from points to patterns including lines, circles, and ellipses by gradient descent. In 2006, Huang *et al.* also adopted the HTNN to detect lines of direct waves and hyperbolas of reflection waves in a one-shot seismogram [7, 8]. The iterative method required less memory, but gradient descent method had local minimum problem.

Simulated annealing (SA) is a global optimization algorithm proposed by Kirkpatrick

Received February 1, 2008; accepted November 28, 2008.
Communicated by Yau-Hwang Kuo, Pau-Choo Chung and Jar-Ferr Yang.
* This work was supported in part by the National Science Council of Taiwan, R.O.C. under grants No. NSC 95-2221-E-009-221 and NSC 96-2221-E-009-197.

in 1983 [9]. The algorithm compares the minimization problem to annealing in metallurgy where careful annealing makes perfect crystal. The key of the algorithm to reach the global minimum is in conditionally accepted higher-energy states by Metropolis criterion [10].

Here, we take the advantage of global optimization in SA to minimize the distance between input points and patterns such as lines, circles, ellipses, and hyperbolas. Also the proposed detection system is applied to the detection of line pattern of direct wave and the hyperbolic pattern of reflection wave in the one-shot seismogram.

In section 2, the proposed system including error definition and the steps of the algorithm is presented. Section 3 shows the experimental results for the simulated image patterns, simulated seismic patterns, and real seismic patterns. Conclusions and discussions are presented in the section 4.

2. SIMULATED ANNEALING PARAMETER DETECTION SYSTEM

We propose the detection system in Fig. 1. The detection system takes the N data as the input, followed by the SA parameter detection system to detect a set of parameter vectors of K patterns. After convergence, patterns are recovered from the detected parameter vectors.

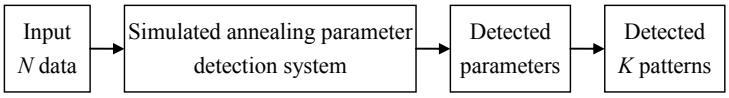

Fig. 1. System overview.

SA parameter detection system consists of two main parts: (1) definition of system error (energy, distance); (2) SA algorithm for determination of the parameter vectors with minimum error. To obtain the system error, we calculate the error or the distance from a point to patterns, and combine the errors from all points to patterns to be the system error.

2.1 Parametric Patterns

Ellipses and hyperbolas with center at (m_x, m_y) and rotation θ in 2-D space can be expressed by the equation using 6 parameters m_x, m_y, a, b, θ, and f as

$$a[(x-m)\cos\theta+(y-m)\sin\theta]+b[-(x-m)\sin\theta+(y-m)\cos\theta]=f. \quad (1)$$

Table 1 lists the relation between the graph of the equation and parameters a, b, and f. If $a > 0$, $b > 0$, and $f > 0$ or $a < 0$, $b < 0$, and $f < 0$, the graph is an ellipse; if $a > 0$, $b < 0$, and $f \neq 0$ or $a < 0$, $b > 0$, and $f \neq 0$ the graph is a hyperbola. If $a > 0$, $b < 0$, and $f = 0$ or $a < 0$, $b > 0$, and $f = 0$, the graph represents the asymptotes of the hyperbola. When $f = 0$, the graph is a set of asymptote of a hyperbola and which are two crossing lines, so we can use Eq. (1) to represent lines.

Table 1. Relation between graph and parameters *a*, *b*, and *f* in Eq. (1).

a	*b*	*f*	Graph
+	+	+	Ellipse
–	–	–	Ellipse
+	–	+	Hyperbola
–	+	+	Hyperbola
+	–	–	Hyperbola
–	+	–	Hyperbola
+	–	0	Asymptote
–	+	0	Asymptote
–	–	+	No graph
+	+	–	No graph
+	+	0	Point
–	–	0	Point

In vector form, a parameter vector, $\mathbf{p} = [m_x, m_y, a, b, \theta, f]^T$ represents a pattern. For the kth pattern, $\mathbf{p}_k = [m_{k,x}, m_{k,y}, a_k, b_k, \theta_k, f_k]^T$, and for all K patterns, the matrix $\mathbf{P} = [\mathbf{p}_1, \mathbf{p}_2, \ldots, \mathbf{p}_K]$ represents all K patterns.

2.2 System Error

To define the error or energy of the system, we first define the distance from a point to a pattern. Then, the error from a point to K patterns is the geometric mean of the distances from the point to all individual patterns. Finally, the system error or energy is the arithmetic mean of the error of N points. The definition is in the following.

2.2.1 Distance from a point to a pattern

Here, the detected patterns include ellipses, circles, hyperbolas, and lines as asymptotes. The distance from a point $\mathbf{x_i} = [x_i, y_i]^T$ to the kth pattern is defined as

$$d_k(\mathbf{x}_i) = |a_k[(x_i - m_{k,x})\cos\theta_k + (y_i - m_{k,y})\sin\theta_k]^2 + b_k[-(x_i - m_{k,x})\sin\theta_k + (y_i - m_{k,y})\cos\theta_k]^2 - f_k|. \tag{2}$$

Distance measure in Eq. (2) has a minimum $d(x_i) = 0$ when $a = 0$, $b = 0$, and $f = 0$. However, these are not our desired parameters. Also, the distance from a point to the pattern is affected by the scale of coefficients. We normalize the parameter b and a by $\sqrt{|ab|}$, *i.e.*, new $b' = b/\sqrt{|ab|}$ and $a' = a/\sqrt{|ab|}$.

2.2.2 Error from a point to *K* patterns

Error or distance from a point to the patterns is defined as the geometric mean of the distances from the point to all patterns. The error or energy of the ith point $\mathbf{x_i}$ is

$$E_i = E(\mathbf{x}_i) = \left[d_1(\mathbf{x}_i)d_2(\mathbf{x}_i)\ldots d_k(\mathbf{x}_i)\ldots d_K(\mathbf{x}_i)\right]^{\frac{1}{K}} \tag{3}$$

where K is the total number of patterns. If the point is on any pattern, the error of this point will be zero. Fig. 2 shows the error of a point to all patterns. The distance layer computes the distance from a point to each pattern by Eq. (2), and the error layer outputs the error from a point to all patterns by Eq. (3).

2.2.3 Error from N points to K patterns

Fig. 3 illustrates the error or energy of the system from N input points to K patterns. The error or energy of the system is defined as the average of the error of points,

$$E = \frac{1}{N}\sum_{i=1}^{N} E_i. \tag{4}$$

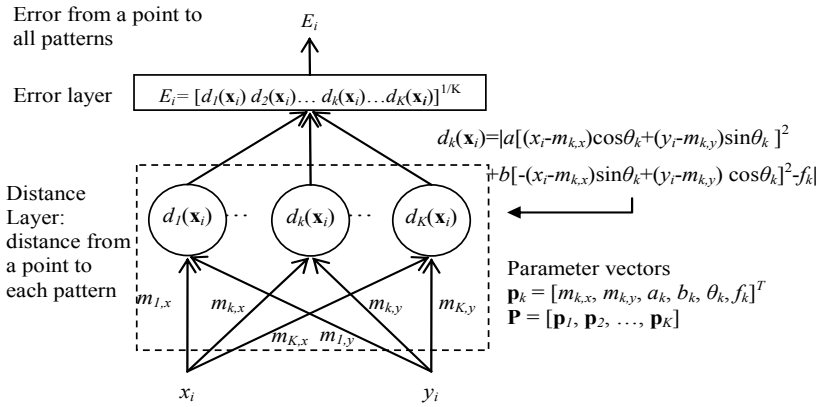

Fig. 2. Distance from a point to all patterns; i is the index of the input point; k is the index of the pattern, and K is the number of patterns.

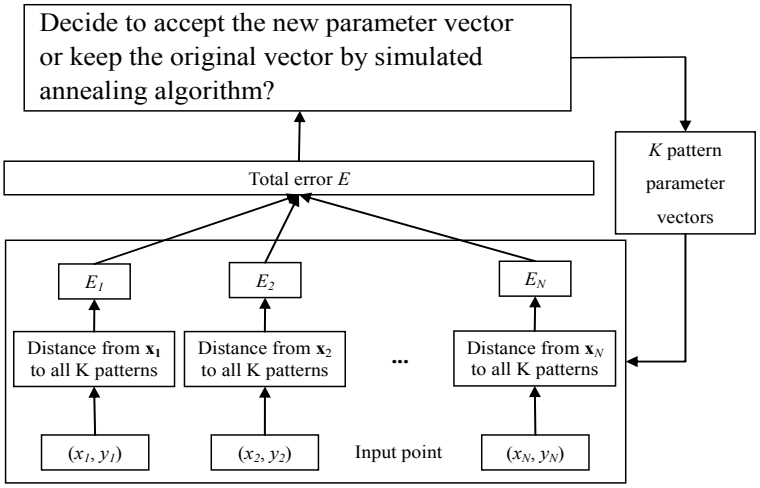

Fig. 3. Total error of the system and procedure of simulated annealing.

2.3 Simulated Annealing for Parameter Detection

We use SA to detect the parameter vector of each pattern. Our goal is to find a set of parameter vectors that can globally minimize the error of the system. Using the temperature decreasing function $T(t)$

$$T(t) = T_{\max} \times 0.98^{(t-1)}, \text{ for } t = 1, 2, 3, \ldots \tag{5}$$

as in [9].

HTNN used gradient descent method in adjusting pattern parameters [6]. Adjusting all parameters at one time was not efficient in convergence [6]. SA is a random adjusting of parameters. It needs more computation in the adjusting parameters than HTNN. So for efficiency, we also use four steps in adjusting parameters. The adjusting order is the center (m_x, m_y), the major and minor axes, b and a, and then the rotation angle θ, followed by the size f. This algorithm is the general algorithm to detect K circles, ellipses, hyperbolas, and it treats lines as asymptotes of hyperbolas, where the number K is preset in the algorithm. In [11], the number of K patterns could be determined by the minimum from the error vs. K.

Algorithm: SA algorithm to detect parameter vectors of K patterns including circles, ellipses, hyperbolas, and lines as asymptotes.
Input: N points in an image. A number K as the number of patterns.
Output: A set of detected K parameter vectors.
Method:
Step 1: Initialization.

In the initial step $t = 1$, choose $T(1) = T_{\max}$ at high temperature, and define the temperature decreasing function as in Eq. (5), $T(t) = T_{\max} \times 0.98^{(t-1)}$. Initialize parameter vectors $p_1, p_2, \ldots, p_k, \ldots, p_K$, where $p_k = [m_{k,x}, m_{k,y}, a_k, b_k, \theta_k, f_k]^T$, one p is for one pattern, and set $P = [p_1, p_2, \ldots, p_k, \ldots, p_K]$. Calculate energy $E(\mathrm{P})$ as Eqs. (2), (3), and (4).

Step 2: Randomly change parameter vectors and decide the new parameter vectors in the same temperature or in one cooling cycle.
For $m = 1$ to N_t (N_t trials in a temperature)
For $k = 1$ to K (k is the index of the pattern)
Start a trial, including steps 2.1 to 2.3 in the following.

Step 2.1: Randomly change the center of the kth pattern:

$$[m'_{k,x} \;\; m'_{k,y}]^T = [m_{k,x} \;\; m_{k,y}]^T + \alpha_m \mathbf{n} \tag{6}$$

where $\mathbf{n} = [n_1 \; n_2]^T$ is a 2×1 random vector, n_1 and n_2 are Gaussian random variables with $N(0, 1)$ and α_m is a constant. Now, $\mathbf{p}_k' = [m'_{k,x}, m'_{k,y}, a_k, b_k, \theta_k, f_k]^T$, and $\mathbf{P}' = [\mathbf{p}_1, \mathbf{p}_2, \ldots, \mathbf{p}'_k, \ldots, \mathbf{p}_K]$.

Calculate the new energy $E(\mathbf{P}')$ from N points to K patterns. Using Metropolis criterion decides whether or not to accept P′: If the new energy is less than or equal to the original one, $\Delta E = E(\mathbf{P}') - E(\mathbf{P}) \leq 0$, accept P′. Otherwise, the new energy is higher than the original one, $\Delta E = E(\mathbf{P}') - E(\mathbf{P}) > 0$. In this case, it computes $prob = \exp[-\Delta E/T(t)]$,

and generates a random number x uniformly distributed over [0, 1]. If $prob \geq x$, accept $\mathbf{P}'$; otherwise, reject it, and keep original $\mathbf{P}$.

Step 2.2: Randomly change the shape parameters:

$$[a_k' \ b_k']^T = [a_k \ b_k]^T + \alpha_{ab}\mathbf{n} \tag{7}$$

and normalize it by $\sqrt{|a_k'b_k'|}$, where $\mathbf{n} = [n_1 \ n_2]^T$ is a 2×1 random vector, n_1 and n_2 are Gaussian random variables with $N(0, 1)$ and α_{ab} is a constant. Now, $\mathbf{p}'_k = [m_{k,x}, m_{k,y}, a_k', b_k', \theta_k, f_k]^T$, and $\mathbf{P}' = [\mathbf{p}_1, \mathbf{p}_2, \ldots, \mathbf{p}'_k, \ldots, \mathbf{p}_K]$. Similar to step 2.1, calculate the new energy $E(\mathbf{P}')$ from N points to K patterns. Using Metropolis criterion decides whether to accept $\mathbf{P}'$, or keep original $\mathbf{P}$.

Step 2.3: Randomly change the angle:

$$\theta_k' = \theta_k + \alpha_\theta n \tag{8}$$

where n is a Gaussian random variable with $N(0, 1)$ and α_θ is a constant. Here, the angle is in degree. Now, $\mathbf{p}'_k = [m_{k,x}, m_{k,y}, a_k, b_k, \theta_k', f_k]^T$, and $\mathbf{P}' = [\mathbf{p}_1, \mathbf{p}_2, \ldots, \mathbf{p}'_k, \ldots, \mathbf{p}_K]$. Similar to step 2.1, calculate the new energy $E(\mathbf{P}')$ from N points to K patterns. Using Metropolis criterion decides whether to accept $\mathbf{P}'$, or keep original $\mathbf{P}$.

Step 2.4: Randomly change the size:

$$f_k' = |f_k + \alpha_f n| \tag{9}$$

where n is a Gaussian random variable with $N(0, 1)$ and α_f is a constant. Now, $\mathbf{p}'_k = [m_{k,x}, m_{k,y}, a_k, b_k, \theta_k, f_k']^T$, and $\mathbf{P}' = [\mathbf{p}_1, \mathbf{p}_2, \ldots, \mathbf{p}'_k, \ldots, \mathbf{p}_K]$. Similar to step 2.1, calculate the new energy $E(\mathbf{P}')$ from N points to K patterns. Using Metropolis criterion decides whether to accept $\mathbf{P}'$, or keep original $\mathbf{P}$.

End for k (pattern)
End for m (trial)

Step 3: Cool the System.

Decrease temperature T according to the cooling function Eq. (5), $T(t) = T_{\max} \times 0.98^{(t-1)}$, for $t = 1, 2, 3, \ldots$, and repeat steps 2 and 3 until the temperature is low enough, for examples, repeat 500 times.

3. EXPERIMENTAL RESULTS

The experiments are first on simulated pattern detections in images with size 50×50. We use the general algorithm to detect hyperbolas, ellipses, and consider lines as asymptotes of hyperbolas. Then, we use the algorithm just for North-South opening hyperbolas in seismic applications. In seismic applications, we detect line pattern of direct wave and hyperbolic pattern of reflection wave in the simulated and real seismic data.

3.1 Detection of Circles, Ellipses, Hyperbolas, and Lines

The general algorithm can detect circles, ellipses, hyperbolas, and treats line as asymptote. In initial stage, m_x and m_y are randomly distributed over [0, 50], $f_k = 0$, $a_k = 1$, $b_k = 1$, and $\theta_k = 0$. The cooling function is as Eq. (5) with a high enough temperature, $T_{\max} = 500$. We have 100 trials in the same temperature. The temperature decreases 500 times to $T = 0.0209$, and this temperature is low enough. Constants $\alpha_m = 1$, $\alpha_{ab} = 1$, $\alpha_\theta = 2$, and $\alpha_f = 2$.

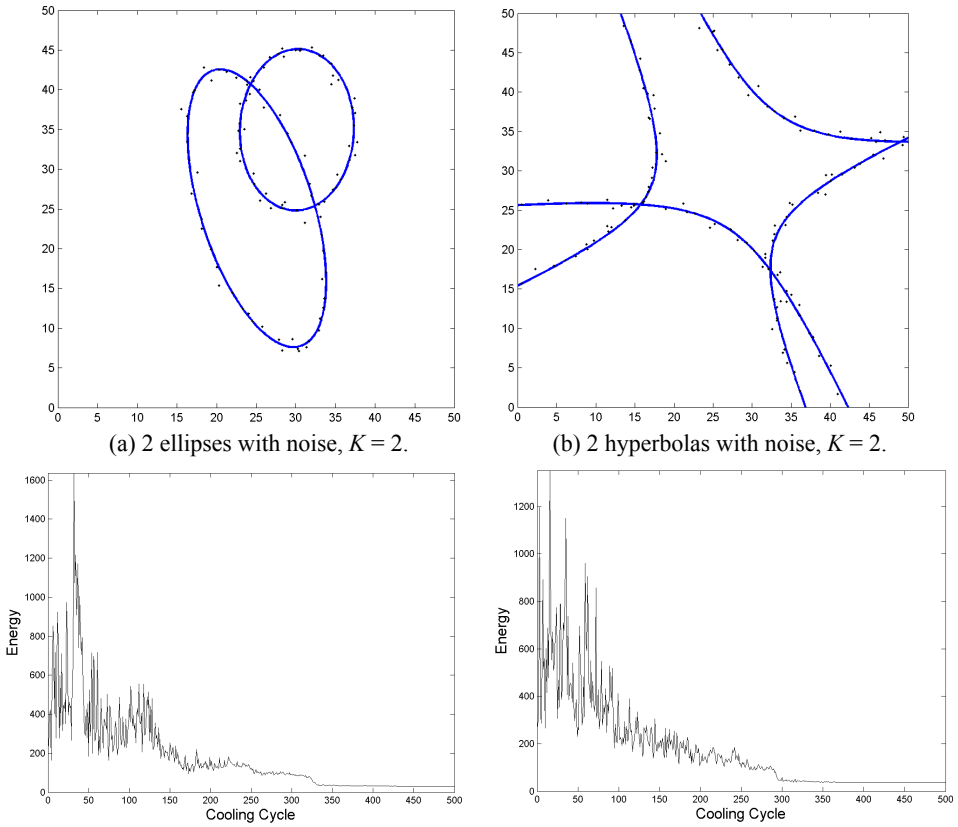

(a) 2 ellipses with noise, $K = 2$. (b) 2 hyperbolas with noise, $K = 2$.

(c) and (d) corresponding plot of energy vs. cooling cycle.

Fig. 4. Detection of ellipses and hyperbolas.

Fig. 4 shows the detection result of ellipses and hyperbolas where $K = 2$. Patterns are with Gaussian noise $N(0, 0.5) \times N(0, 0.5)$. Figures of energy vs. cooling cycles are also shown. Fig. 5 shows the detection result of mixed ellipse, hyperbola, and line in an image. In Figs. 5 (b) and (c), the detected line is a hyperbola with small size. In Fig. 5 (d), since an asymptote is a pair of crossing lines, we set $K = 1$ and $f = 0$ and use this to detect two crossing lines.

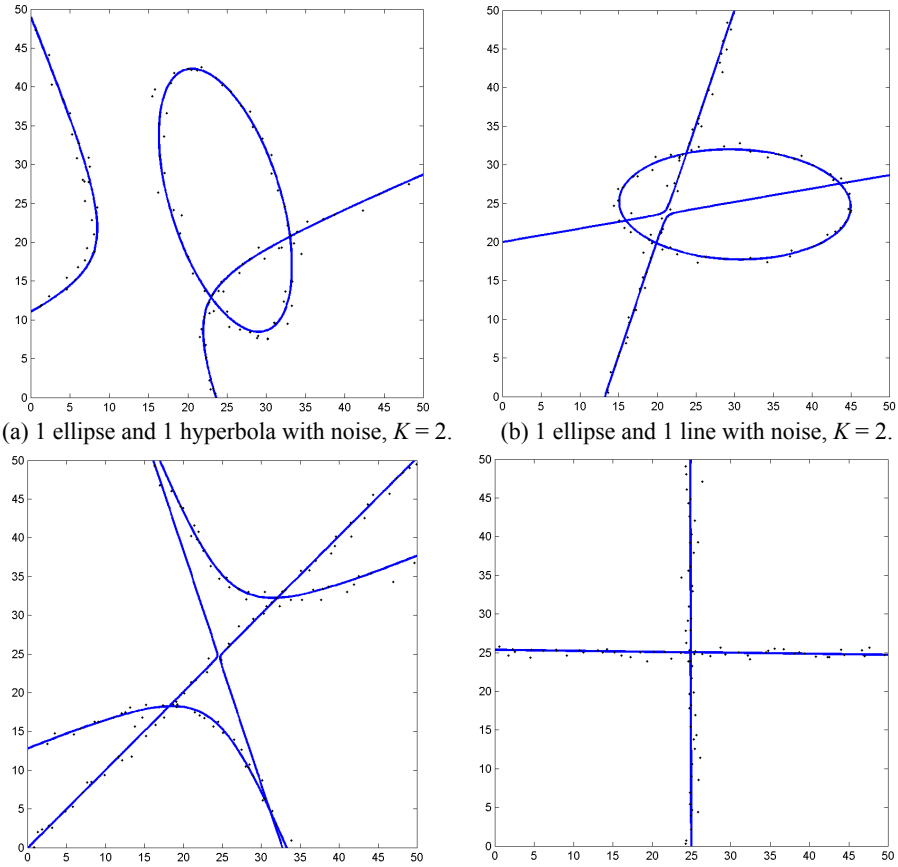

(a) 1 ellipse and 1 hyperbola with noise, $K = 2$. (b) 1 ellipse and 1 line with noise, $K = 2$.

(c) 1 hyperbola and 1 line with noise, $K = 2$. (d) 2 lines with noise, $K = 1, f = 0$.

Fig. 5. Detection of ellipses, hyperbolas, and lines.

3.2 Seismic Applications

In a seismogram, the line pattern of direct wave and hyperbolic pattern of reflection wave are always North-South opening [2-4]. The equation is

$$a(x - m_x)^2 + b(y - m_y)^2 = f \tag{10}$$

with $a < 0$, $b > 0$, and $f \geq 0$. Five parameters $\mathrm{p} = [m_x, m_y, a, b, f]^T$ represents a pattern. In the algorithm, there are three steps in adjusting parameters. The adjusting order is the center (m_x, m_y), the major and minor axes, b and a, followed by the size f.

3.2.1 Experiments on simulated one-shot seismogram

In simulated seismic application, experiment is on horizontal reflection layer. Two lines are the asymptote of the hyperbola [2-4], and the asymptote is a hyperbola with size zero. So a line can be treated as a hyperbola.

Fig. 6 is the shot-receiver relation. An exploration or a shot is produced at the middle and several receiving stations locate along the line of both sides expand from the exploration. The distance between the shot and the receiving station is x. The depth of layer is h. The velocity of p-wave is v. The travelling time formula is hyperbolic as Eq. (11).

$$\left(\frac{2h}{v}\right)^2 + \left(\frac{x}{v}\right)^2 = t^2 \tag{11}$$

For the direct wave, the time-distance curve is a line.

$$t = \frac{x}{v} \tag{12}$$

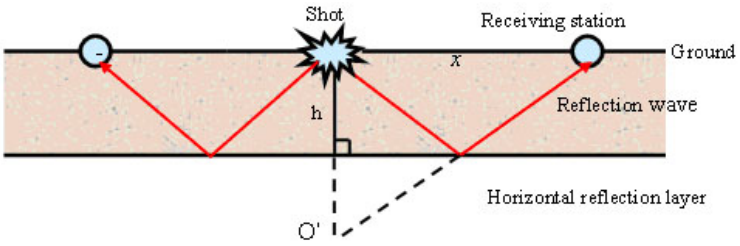

Fig. 6. Shot-receiver relation.

The simulated horizontal reflection layer in Fig. 6 is with the depth 500 m and the velocity of the p-wave in the sedimentary rock is 2,500m/sec. There are 65 receiving stations with 50 m between each other, the shot is in the middle. The sampling interval is 0.004 sec. The impulse response is 25 Hz Ricker wavelet. Reflection coefficient is 0.2 and noise is band-passed, 10.2539Hz ~ 59.5703Hz, with uniform distributed over [– 0.2, 0.2]. Fig. 7 (a) shows the one-shot seismogram from Fig. 6. The horizontal axis is the trace number and the vertical axis stands for time t. The one-shot seismogram is first preprocessed by envelope processing, thresholding, and peak detection [5] and shown in Fig. 7 (b) with the threshold 0.15. The image size is 512 × 65. The points are then used as the input to the parameter detection system.

The initial parameter $m_{k,x}$ and $m_{k,y}$ are random between 0 and 50, $a_k = -1$, $b_k = 1$, and $f_k = 1$. The cooling function is as Eq. (5) with a high enough temperature, $T_{\max} = 600$. There are $N_t = 100$ trials in a temperature. The temperature decreases 500 times. Constants $\alpha_m = 1$, $\alpha_{ab} = 0.5$, and $\alpha_f = 5$. Since lines of direct wave is asymptotes of a hyperbola, we set $f_1 = 0$. The detection result and the error plot of Fig. 7 are shown in Figs. 8 (a) and (b). Table 2 lists the detected parameters in Fig. 8 (a).

Table 2. Detected parameters in Fig. 8 (a) in image space 512 × 65.

	m_x	m_y	a	b	f
Direct wave	33.0	8.2	– 5.0	0.2	0 (preset)
Reflection wave	32.9	40.1	– 4.4	0.2	1040.9

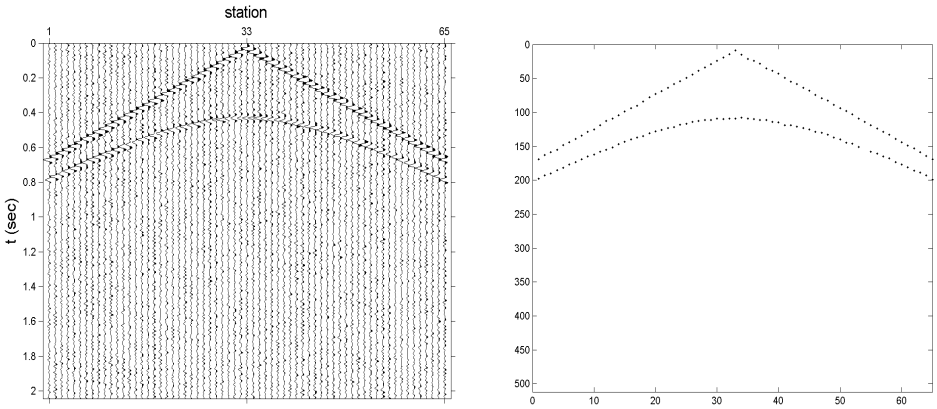

(a) Simulated one-shot seismogram (horizontal reflection layer). (b) After envelope and peak detection.

Fig. 7. Simulated seismic patterns.

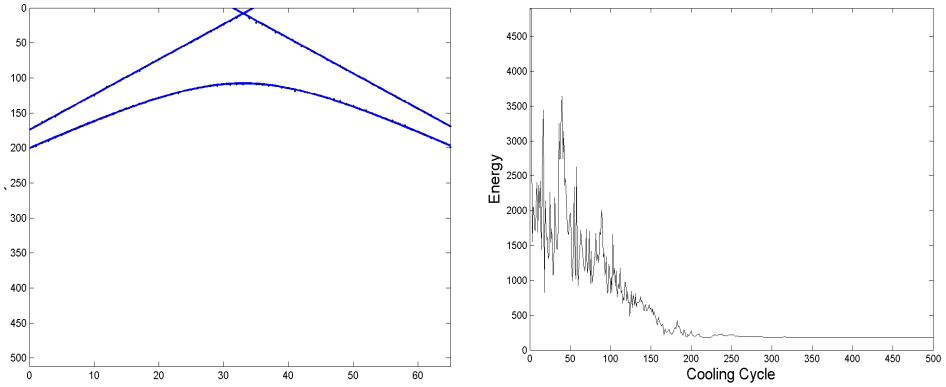

(a) Detection result. (b) Energy vs. cooling cycle.

Fig. 8. Detection of simulated seismic patterns in Fig. 7.

3.2.2 Experiments on real one-shot seismogram

The system is also applied to detect direct wave and reflection wave in real seismic data. We obtain data from Seismic Unix System developed by Colorado School of Mine [4].

The real data showed in Fig. 9 is at Canadian Artic, which has 48 traces and 3100 samples per trace with sampling interval 0.002 seconds. The horizontal axis is the trace number and the vertical axis is time t.

After preprocessing of envelope processing, thresholding, and peak detection [5], we only choose points with $t < 1.4$ seconds which includes points from direct wave, first reflection wave, and second reflection wave as in Fig. 10 (a), where there are 88 points. The detection result is shown in Fig. 10 (b). Table 3 lists the detected parameters in image space $3{,}100 \times 48$.

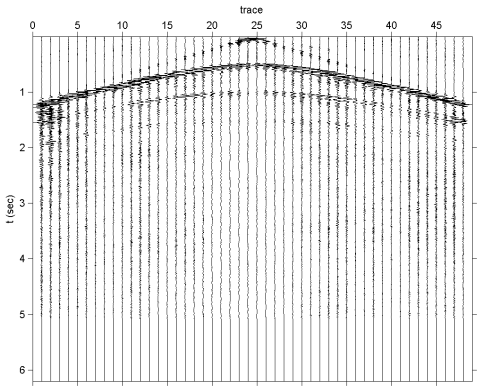

Fig. 9. Real seismic data at Canadian Artic.

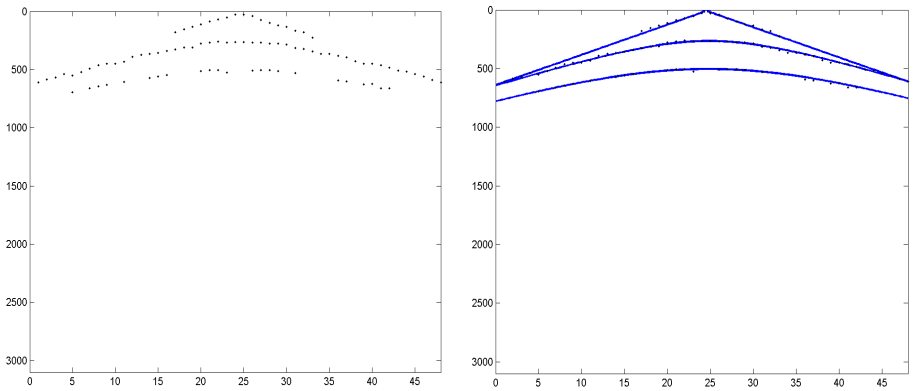

(a) (b)

Fig. 10. (a) After envelope and threshold preprocessing, choose peaks with $t < 1.4$ sec.; (b) Detection result of seismic patterns in (a).

Table 3. Detected parameters in Fig. 10 (b) with fixed $f_1 = 0$ in image space 3,100 × 48.

	m_x	m_y	a	b	f
Direct wave	24.5	8.6	– 25.7	0.04	0 (preset)
Reflection wave	24.8	28.8	– 22.9	0.04	2,441.7
Second reflection wave	24.7	49.6	– 23.1	0.04	8,942.7

4. CONCLUSIONS AND DISCUSSIONS

We have proposed a pattern detection system, which adopts the simulated annealing algorithm to detect patterns such as lines, circles, ellipses, and hyperbolas by finding their parameters in an unsupervised manner and global minimum fitting error between N points and K patterns in an image. We define the distance from a point to a pattern and this makes the computation feasible, especially for hyperbola. The system error between N points and K patterns is defined. Using four steps to adjust parameters from center,

shape, angle, to the size of the pattern can get fast convergence. Experimental results on the detection of circles, ellipses, hyperbolas, and lines in images are successful. The detection results of line pattern of direct wave and hyperbolic pattern of reflection wave in simulated and real one-shot seismogram are good and can improve seismic interpretations and further seismic data processing. The detected parameters of lines and hyperbolas help geophysicists to estimate the *p*-wave velocity, the depth of the reflection layer and the dipping angle.

For the cooling schedule, the value of initial temperature T_{max}, and the number of trials in one temperature N_t have been tested many times. The used value in this study can get good performance in the experiments.

In seismic pattern detection, we have no constraint on the center. However, for ideal case, the hyperbola has the center on x-axis, *i.e.* $t = 0$. In the detection result of simulated seismic data, we can find that the center is not on the x-axis, because convolution produces a shift. So preprocessing is quite critical. Wavelet and deconvolution processing may be needed in the preprocessing to improve the detection result.

ACKNOWLEDGEMENTS

The authors would like to thank the Colorado School of Mines for the use of Seismic Unix System and the real data. The authors also thank Mr. Ying-Liang Chou for his formatting the manuscript.

REFERENCES

1. P. V. C. Hough, "Method and means for recognizing complex patterns," U.S. Patent 3069654, 1962.
2. M. M. Slotnick, *Lessons in Seismic Computing*, the Society of Exploration Geophysicists, Tulsa, 1959.
3. M. B. Dobrin and C. H. Savit, *Introduction to Geophysical Prospecting*, McGraw-Hill Book Co., New York, 1988.
4. O. Yilmaz, *Seismic Data Processing*, the Society of Exploration Geophysicists, Tulsa, 1987.
5. K. Y. Huang, K. S. Fu, T. H. Sheen, and S. W. Cheng, "Image processing of seismograms: (A) Hough transformation for the detection of seismic patterns; (B) Thinning processing in the seismogram," *Pattern Recognition*, Vol. 18, 1985, pp. 429-440.
6. J. Basak and A. Das, "Hough transform networks: Learning conoidal structures in a connectionist framework," *IEEE Transactions on Neural Networks*, Vol. 13, 2002, pp. 381-392.
7. K. Y. Huang, J. D. You, K. J. Chen, H. L. Lai, and A. J. Don, "Hough transform neural network for seismic pattern detection," in *Proceedings of International Joint Conference on Neural Networks*, 2006, pp. 4670-4675.
8. K. Y. Huang, K. J. Chen, J. D. You, and A. C. Tung, "Hough transform neural network for pattern detection and seismic applications," *Neurocomputing*, Vol. 71, 2008, pp. 3264-3274.

9. S. Kirkpatrick, C. D. Gelatt, and M. P. Vecchi, "Optimization by simulated annealing," *Science*, Vol. 220, 1983, pp. 671-680.
10. N. Metropolis, A. Rosenbluth, M. Rosenbluth, A. Teller, and E. Teller, "Equation of state calculations by fast computing machines," *Journal of Chemical Physics*, 1953, pp. 1087-1092.
11. K. J. Chen, "Simulated annealing for pattern detection and seismic applications," Master Thesis, Department of Computer Science, National Chiao Tung University, 2007.

Kou-Yuan Huang (黃國源) received the B.S. in Physics (1973) and M.S. in Geophysics (1977) from the National Central University, Taiwan, and M.S.E.E. (1980) and Ph.D. in Electrical and Computer Engineering (1983) from Purdue University. From September 1983 to August 1988, he joined the faculty in the Department of Computer Science, University of Houston-University Park. Now he is the Professor at the Department of Computer Science at National Chiao Tung University, Hsinchu, Taiwan. He widely published papers in journals: Geophysics, Geoexploration, Pattern Recognition, IEEE Transactions on Geoscience and Remote Sensing, Neurocomputing, Computer Processing of Oriental Languages, …, *etc*. He has authored two books, Neural Networks and Pattern Recognition, Weikeg Publishing Co., Taipei, Taiwan, 2000, 2nd ed., 2003, and Syntactic Pattern Recognition for Seismic Oil Exploration, World Scientific Publishing Co., Singapore, in Series in Machine Perceptron and Artificial Intelligence, Vol. 46, 2002. His major contributions are in the areas of seismic pattern recognition using signal and image processing, statistical, syntactic, neural networks, fuzzy logic, and genetic methods.

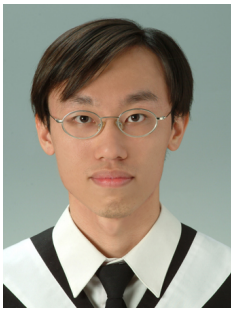

Kai-Ju Chen (陳楷儒) received the B.S. in Computer Science (2005) and M.S. in Multimedia Engineering (2007) from the National Chiao Tung University, Taiwan. His research interests are neural networks, pattern recognition, and signal processing.